Supporting Information

A Noble-Metal-Free Hydrogen Evolution Catalyst Grafted to Visible Light-Absorbing Semiconductors

Gary F. Moore*, Ian D. Sharp*

Joint Center for Artificial Photosynthesis (JCAP), Lawrence Berkeley National Laboratory, Berkeley, California 94720, USA.

Materials

Single crystalline (111) Si and (100) GaP wafers were purchased from University Wafer. The Si wafers were *p*-type doped with B, yielding a resistivity of 1 – 2 Ω·cm. The GaP wafers were *p*-type doped with Zn, yielding a resistivity of 0.3 Ω·cm. Both materials were single side polished to an epi-ready finish. Diced semiconductor samples were degreased by sonication in acetone and isopropanol for 5 min each, followed by drying under flowing nitrogen. Samples were then exposed to an air-generated oxygen plasma (Harrick Plasma, USA) at 30 W for 5 min. Surface oxide layers were then removed by immersion of the plasma-treated samples in buffered hydrofluoric acid (7:1 HF:NH_4F in H_2O) for 5 min, followed by rinsing in DI water (Milli-Q, 18.2 MΩ·cm) and drying under flowing nitrogen.

Instruments

FTIR. Grazing angle attenuated total reflection Fourier transform infrared spectroscopy (GATR-FTIR) was performed using a VariGATR accessory (Harrick Scientific) with a Ge crystal plate installed in a Bruker Vertex 70. Samples were pressed against the Ge crystal in order to ensure effective optical coupling. Spectra were collected under a dry nitrogen purge with a 4 cm^{-1} resolution, GloBar MIR source, a broadband KBr beamsplitter, and a liquid nitrogen cooled MCT detector. Background measurements were obtained from the bare Ge crystal. Spectra from model compounds in pressed KBr pellets were performed with the same settings in transmission mode.

XPS. X-ray photoelectron spectroscopy was performed using a monochromatized Al Kα source (hν = 1486.6 eV), operated at 150 W, on a Kratos Axis Ultra DLD system at a takeoff angle of 0º relative to the surface normal, and pass energy of 20 eV, corresponding to an instrument resolution of approximately 600 meV. Spectral fitting was achieved using Casa XPS analysis software. Spectral positions were corrected by shifting the primary C 1s core level position to 284.8 eV and curves were fit with quasi-Voigt lines following Shirley background subtraction.

UV-VIS-NIR. Spectra were recorded on a Shimadzu SolidSpec-3700 spectrometer with a D_2 (deuterium) lamp for the ultraviolet range and a WI (halogen) lamp for the visible and near-infrared. Transmission and reflectance measurements were performed with an integrating sphere.

NMR. Spectra were recorded on a Bruker 500'54 Ascend spectrometer operating at 500 MHz. Unless otherwise stated, all spectra were collected at room temperature.

Electrochemistry. Cyclic voltammetry was performed with a Biologic potentiostat using a glassy carbon (3 mm diameter) disc working electrode, a platinum counter electrode, and a silver wire pseudoreference electrode in a conventional three-electrode cell. Anhydrous acetonitrile (Aldrich) was used as the solvent for electrochemical measurements. The supporting electrolyte was 0.10 M tetrabutylammonium hexafluorophosphate. The solution was deoxygenated by bubbling with argon. The working electrode was cleaned between experiments by polishing with alumina (50 nm dia.) slurry, followed by solvent rinses. The concentration of the electroactive compound was maintained between 4×10^{-4} M and 8×10^{-4} M. The potential of the pseudoreference electrode was determined using the ferrocenium/ferrocene redox couple as an internal standard (with $E_{1/2}$ taken as 0.40 V vs. NHE).[2] The voltammograms were recorded at sweep rates of 100 mV s^{-1}.

Synthesis

All synthesis was carried out under an argon atmosphere using Schlenk techniques or in a nitrogen glove box. All reagents were purchased from Aldrich. Dichloromethane was purified by distillation over calcium hydride. All solvents were stored over the appropriate molecular sieves prior to use. MilliQ water (18.2 MΩ·cm) was used to prepare all aqueous solutions. The nickel complex **2(**$BF_4)_2$ was prepared according to a previously reported procedure.[1]

Synthesis of N-Allyl-2,2,2-trifluoro-acetamide (1)

Allylamine (25 mL, 334.1 mmol) was added dropwise to a cooled solution (0^o C) of ethyl trifluoroacetate (45 mL, 378.6 mmol) in THF (80 mL). The reaction was allowed to warm to room temperature then stirred for 1h. The reaction mixture was concentrated under reduced pressure and the residue was purified by vacuum distillation using a 15 cm Vigreaux column to give 1 as a colorless oil. ^{1}H NMR (500 MHz, $CDCl_3$) δ 6.42 (br s, 1H), 5.79-5.89 (m, 1H), 5.23-5.29 (m, 2H), 3.98 (t, J=5.6 Hz, 2H). ^{19}F CPD NMR (500 MHz, $CDCl_3$) δ -75.90 (s, 3F)

Synthesis of Trifluro-acetamide Terminated Semiconductor Surfaces.

Freshly cleaned and etched (see material section) single crystalline (111) Si or (100) GaP wafers were placed in quartz flask and covered with N-Allyl-2,2,2-trifluoro-acetamide. The flask was illuminated with UV light (254nm, SPECTROLINE(R) E-SERIES UV LAMP) for 2 h. The modified wafers were then sonicated and washed with isopropanol before drying under nitrogen.

Synthesis of Amine Terminated Semiconductor Surfaces.

Trifluro-acetamide terminated wafers of single crystalline (111) Si or (100) GaP were refluxed in a degassed HCl solution (0.36 M in methanol) for 4 h to deprotect the amine group. The modified wafers were then washed with isopropanol and rinsed with DI water before drying under nitrogen.

Synthesis of Ni Complex Terminated Semiconductor Surfaces.

Amine terminated wafers of single crystalline (111) Si or (100) GaP were dipped in a solution of **2(**$BF_4)_2$ **(**0.5 mM in dichloromethane) in presence of triethylamine (2 mM in dichloromethane) overnight. The modified wafers were rinsed with dichloromethane, acetone and ethanol before drying under nitrogen.

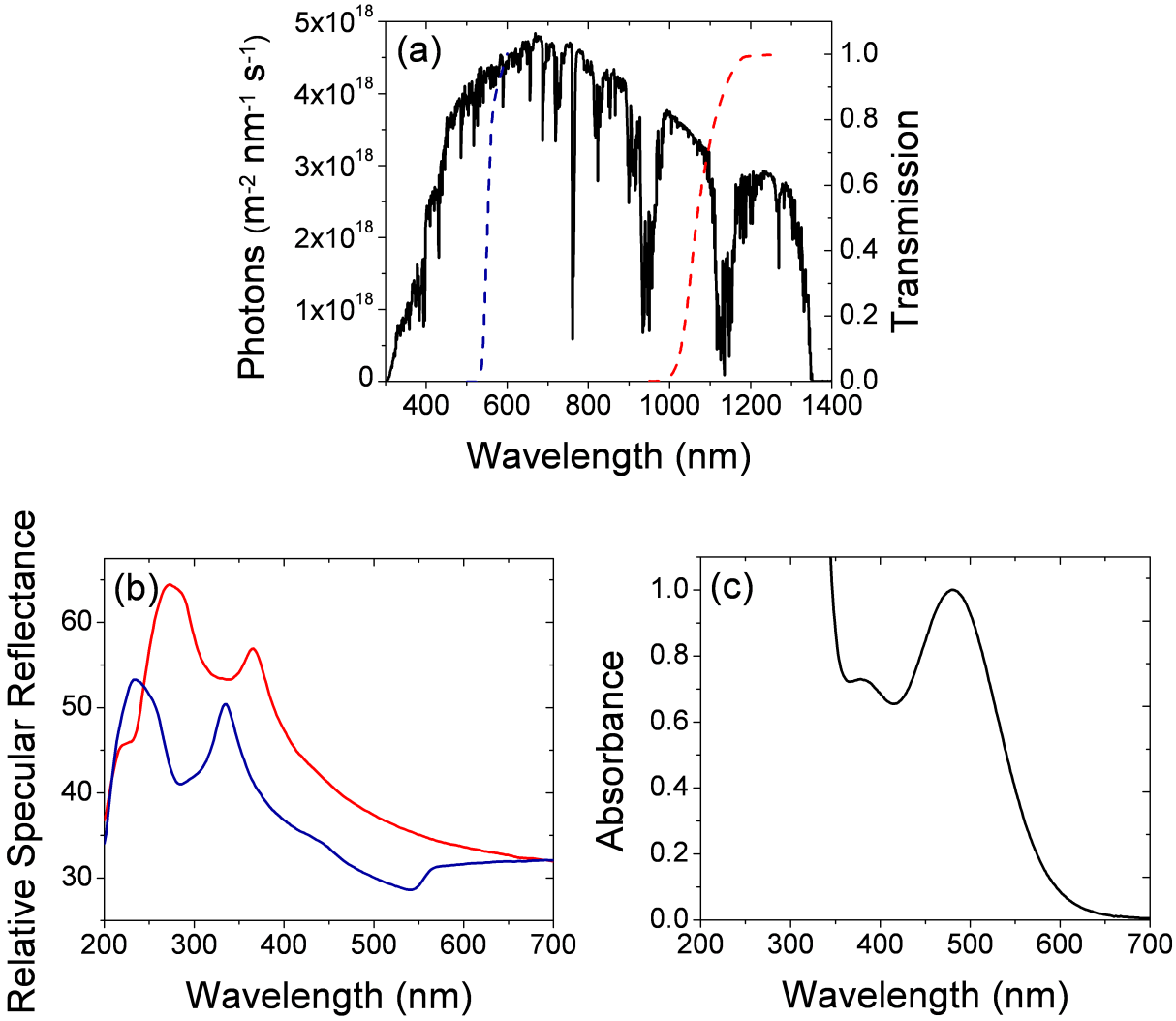

Figure S1. Material optical properties including (a) transmission spectra of (111) Si (red dash) and (100) GaP (blue dash) as well as the AM 1.5 solar flux spectrum (black line), (b) relative specular reflectance spectra of (111) Si (red line) and (100) GaP (blue line) as well as (c) absorbance spectrum of **2**$(BF_4)_2$ in acetonitrile.

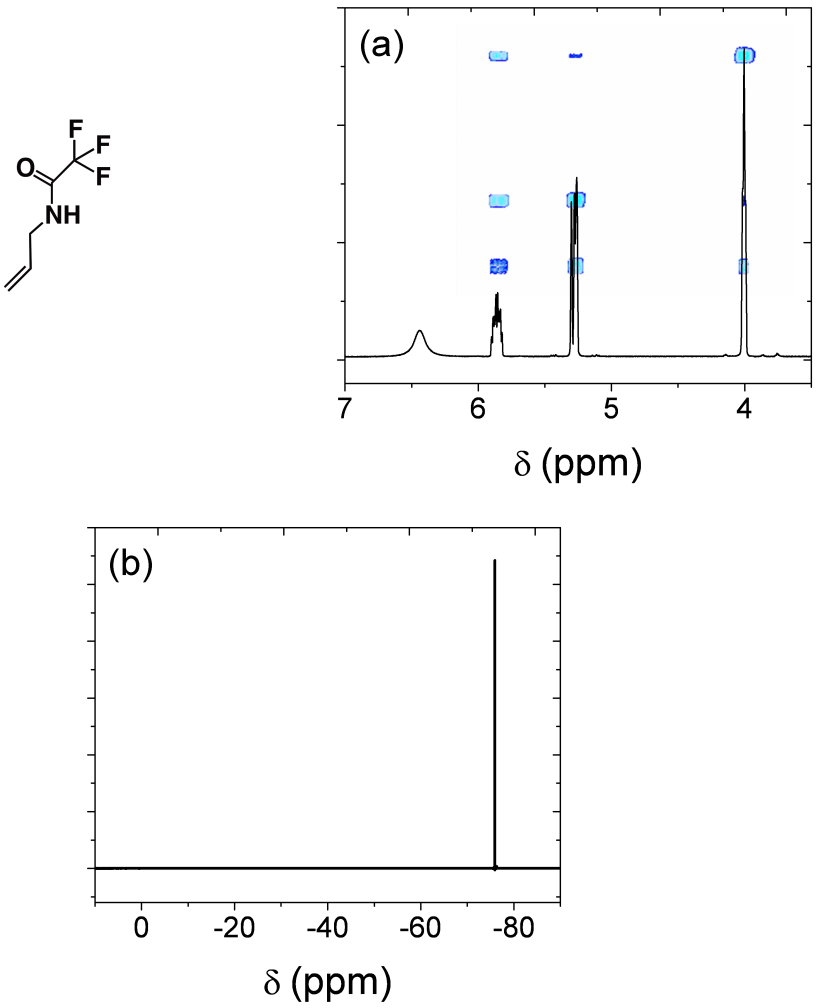

Figure S2. (a) ^{1}H NMR (black line), with overlaid COSY (blue lines), and (b) ^{19}F spectra of N-Allyl-2,2,2-trifluoro-acetamide (**1**) in chloroform-d.

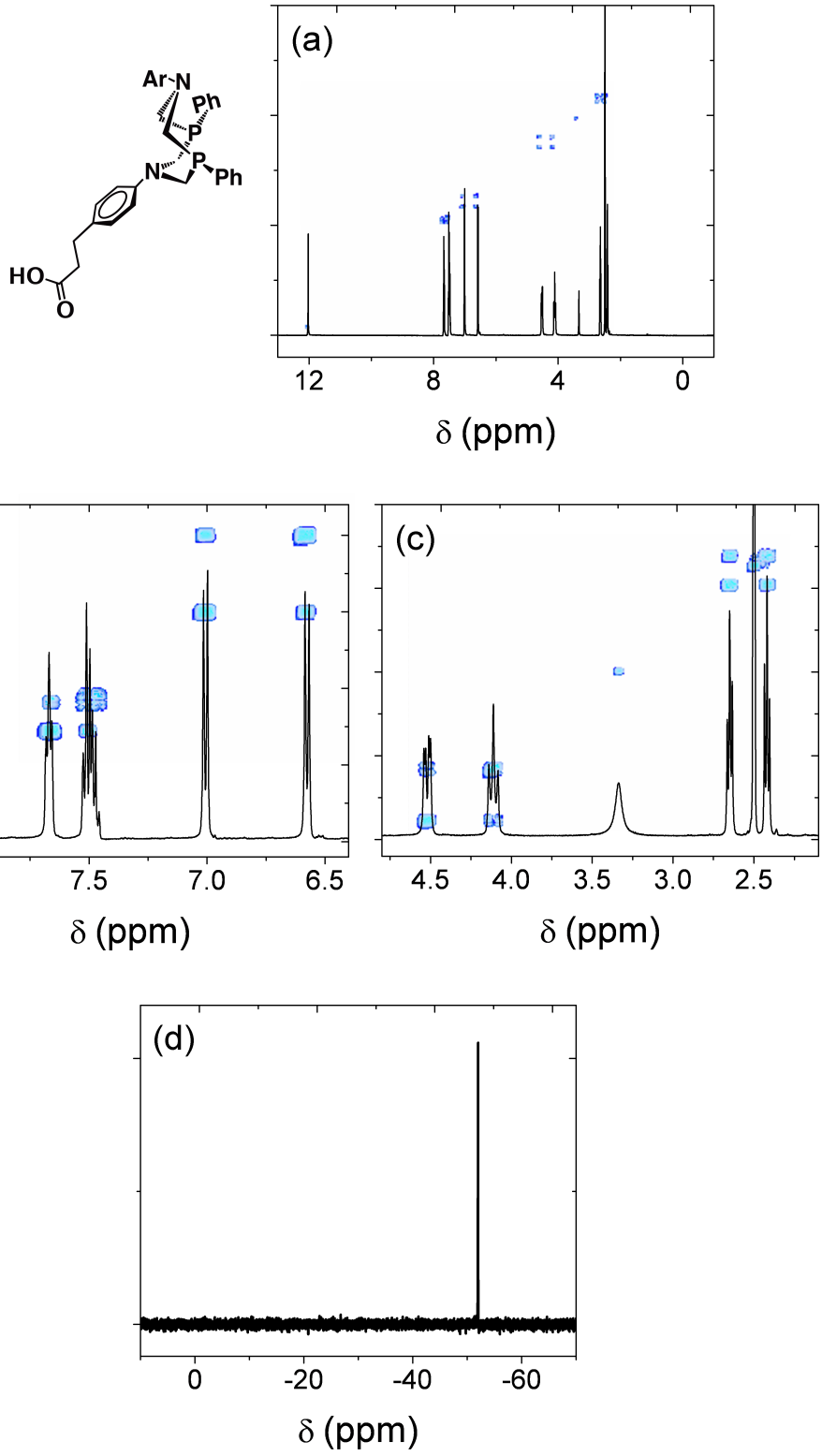

Figure S3. (a, b and c) ^{1}H NMR (black line), with overlaid COSY (blue lines), and (d) ^{31}P spectra of $P^{Ph}{}_2N^{CH2CH2COOH}{}_2$ in dimethyl sulfoxide-d6.

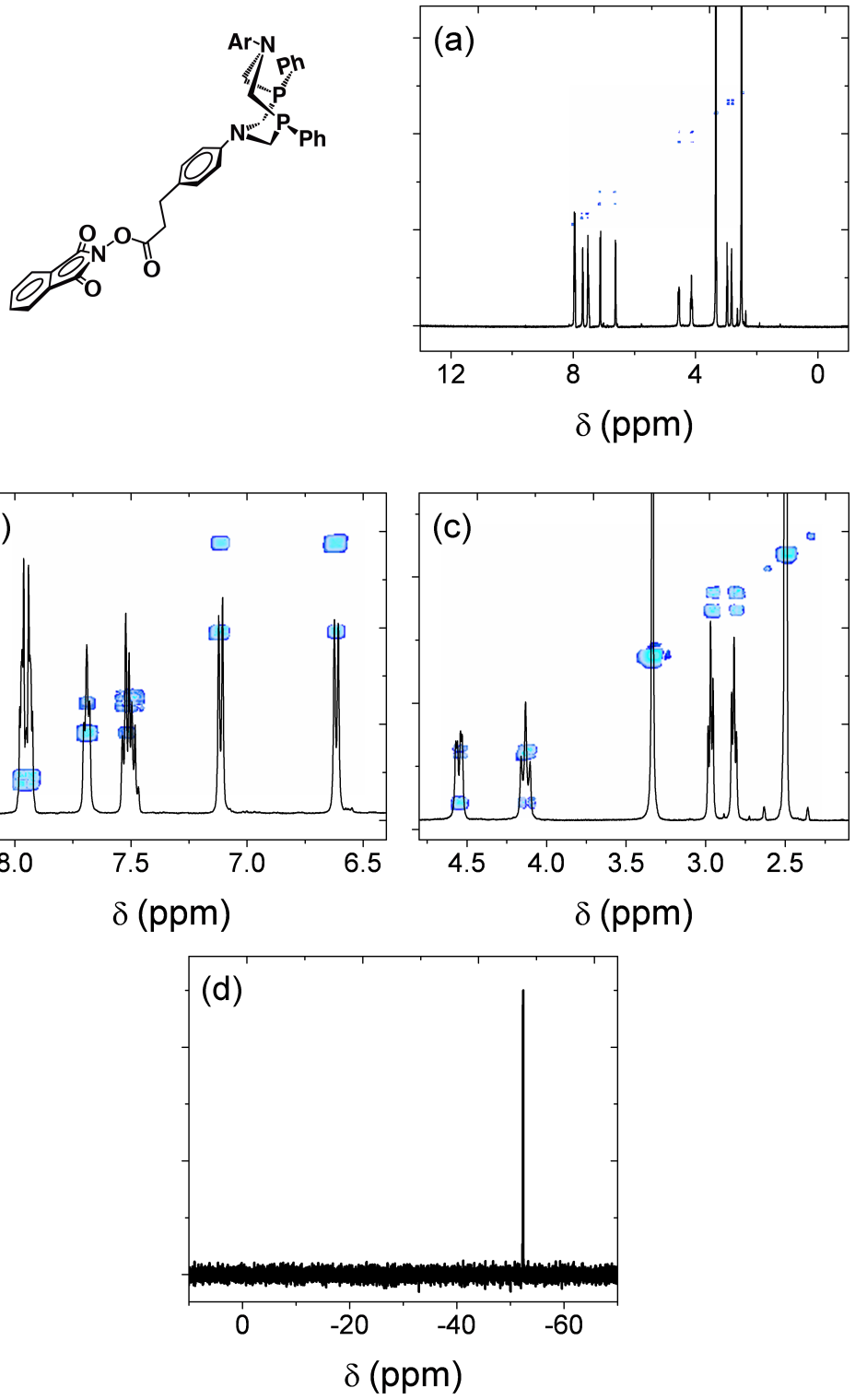

Figure S4. (a, b and c) ^{1}H NMR (black line), with overlaid COSY (blue lines), and (d) ^{31}P spectra of $P^{Ph}{}_2N^{CH2CH2Pth}{}_2$ in dimethyl sulfoxide-d6.

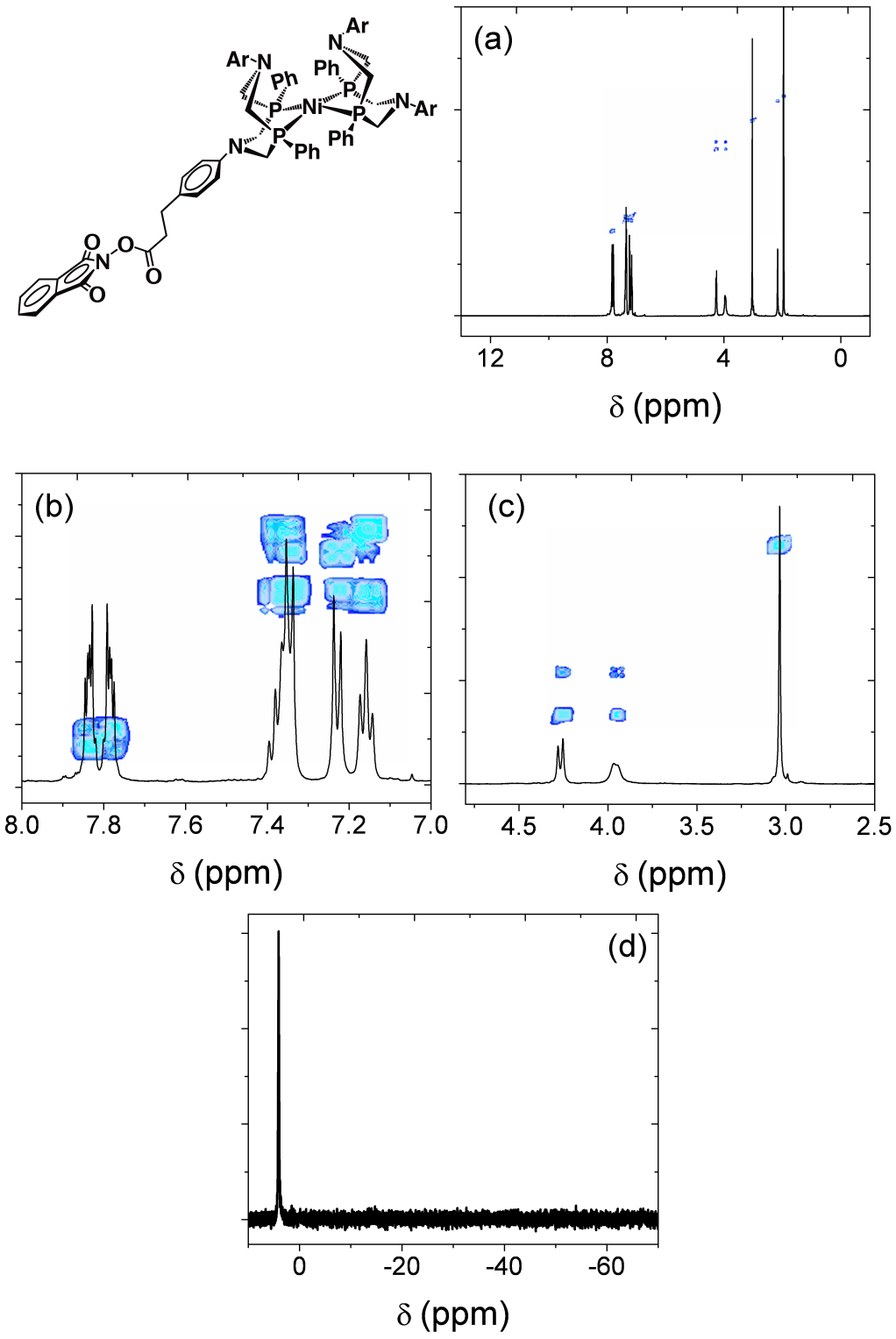

Figure S5. (a, b and c) ^{1}H NMR (black line), with overlaid COSY (blue lines), and (d) ^{31}P spectra of **2**$(BF_4)_2$ in acetonitrile-d3.

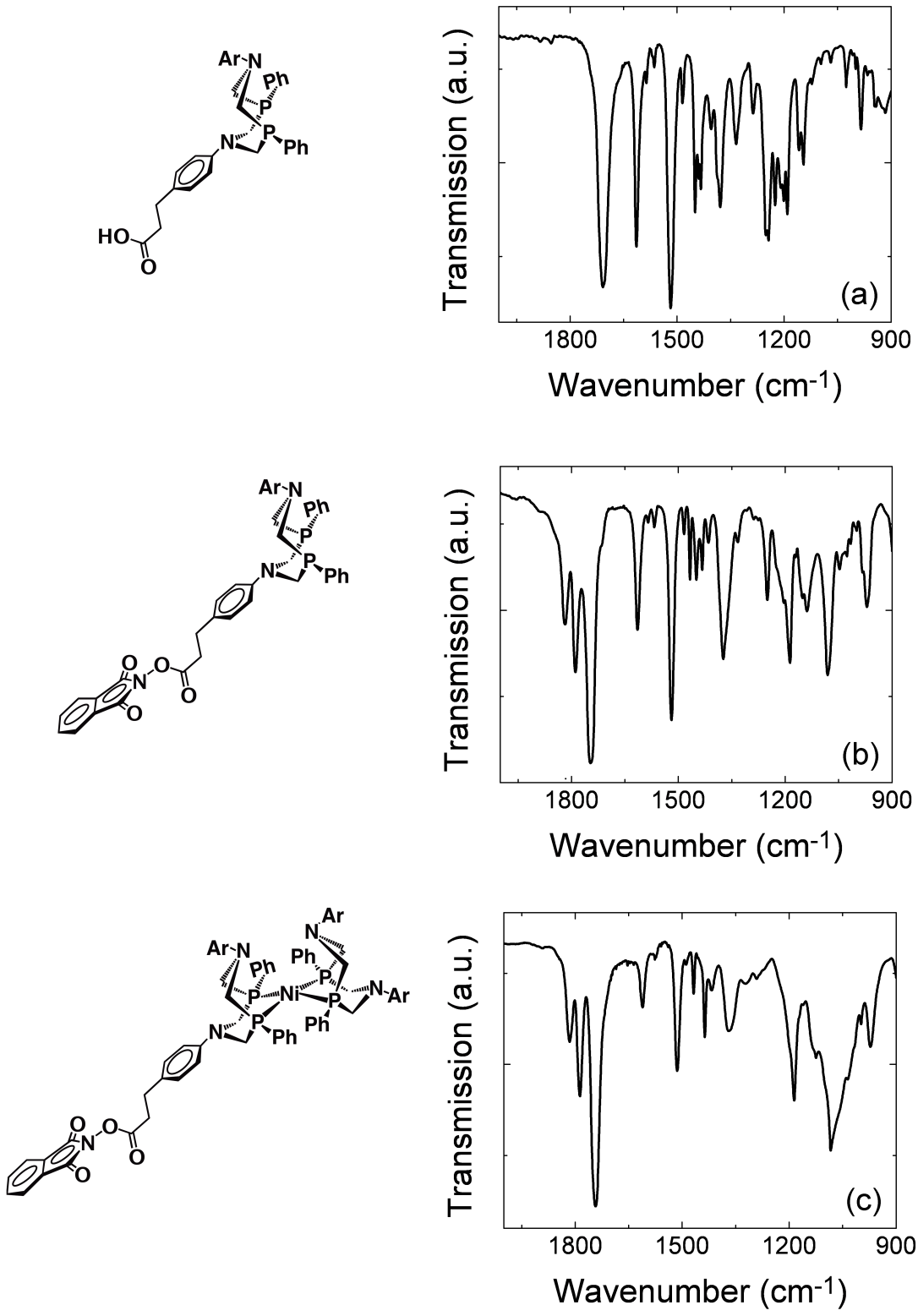

Figure S6. FTIR spectra of (a) $P^{Ph}{}_2N^{CH2CH2COOH}{}_2$, (b) $P^{Ph}{}_2N^{CH2CH2Pth}{}_2$ and **2**$(BF_4)_2$ in KBr.

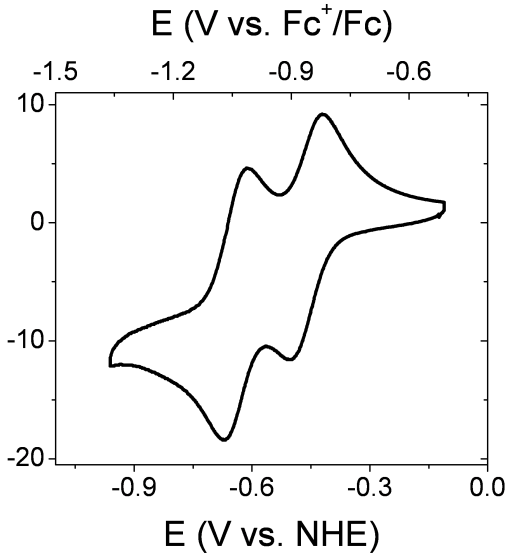

Figure S7. Cyclic voltammogram of **2**$(BF_4)_2$ recorded in a 0.1 M $TBAPF_6$ acetonitrile solution at a scan rate of 100 mV/s, with a glassy carbon working electrode at room temperature.

Compound	$^{II}E_{1/2}$	$^{I}E_{1/2}$
2$(BF_4)_2$	-0.64 V (ΔEp = 60 mV)	-0.46 V (ΔEp = 70 mV)

Table S1. Redox potentials (V vs. NHE) for reduction (^{n}E) of **2**$(BF_4)_2$, as determined by cyclic voltammetry. The electrolyte was 0.1 M tetrabutylammonium hexafluorophosphate in acetonitrile, and the scan rate was 100 mV s^{-1}. Peak-to-peak separations of the observed redox couples (ΔEp) are reported in parenthesis.

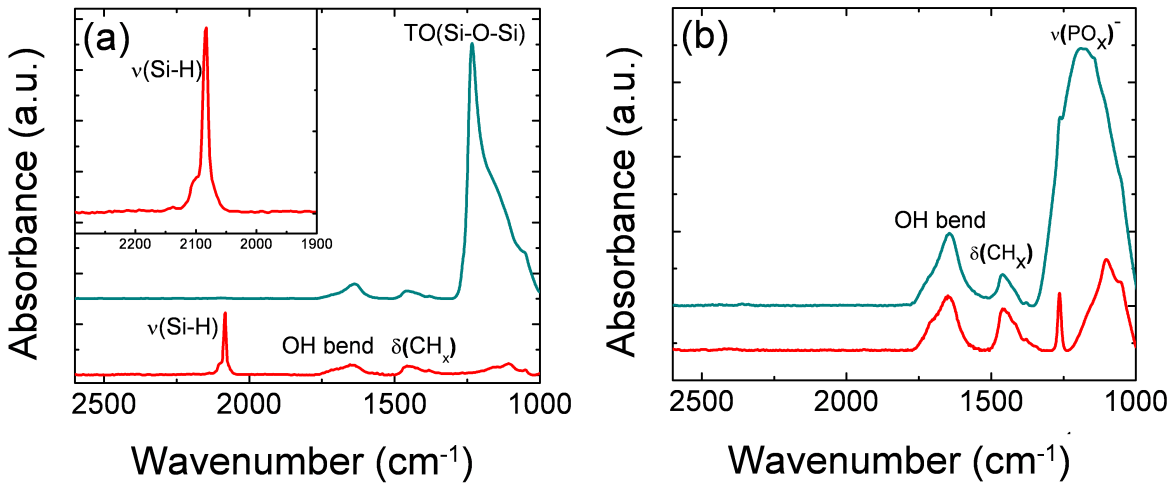

Figure S8. GATR-FTIR spectra of (a) (111) Si as well as (b) (100) GaP obtained before (teal lines) and after (red lines) BHF treatment. Prior to BHF treatment, oxide-related vibrational modes are observed on both materials. Due to air exposure, spectral features associated with OH bending and $\delta(CH_x)$ modes are observed on all samples. The inset of (a) shows the Si-H stretch region, which indicates a monohydride termination of the BHF treated (111) Si surface.

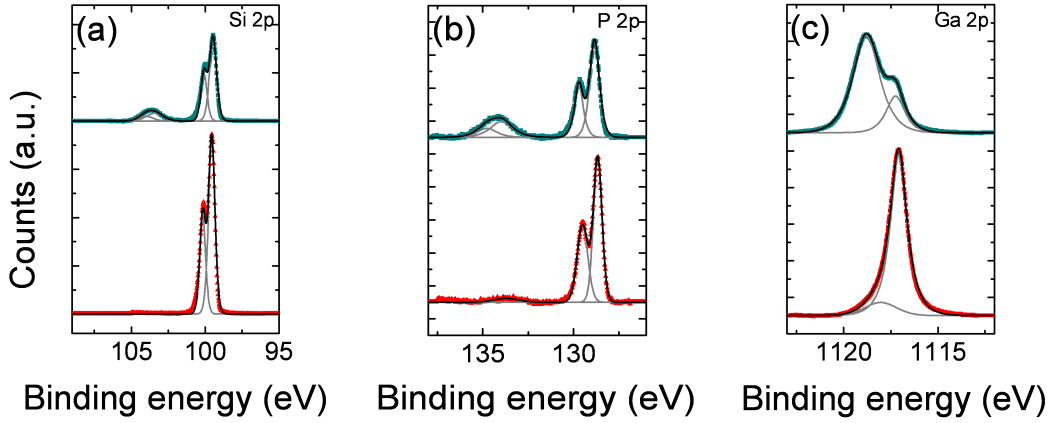

Figure S9. Core level XPS spectra of (a) (111) Si as well as (b and c) (100) GaP obtained before (teal squares) and after (red triangles) BHF treatment. The solid gray and solid black lines are the component and overall fits, respectively. The Si 2p region (a) includes the spin orbit split components from Si^0 of the substrate near 100 eV. The peak near 104 eV associated with Si^{4+} of the surface oxide layer is completely removed by treatment with BHF. The P 2p region (b) is characterized by spin orbit split components near 129 eV from P bound to Ga in the substrate, as well as an oxide component near 134 eV. Likewise, the Ga $2p_{3/2}$ region (c) includes a component near 117 eV from Ga bound to P in the substrate, as well as at 119 eV from Ga bound to O. These results indicate that BHF treatment leads to a significant reduction of the oxide-related components from GaP substrate core level regions. However, remnant bonding of both P and Ga to O is observed, as described in the main text.

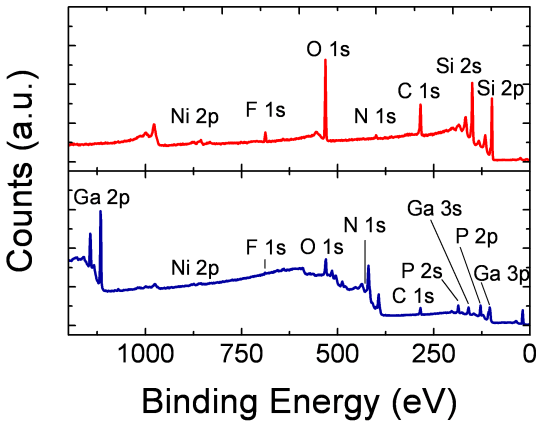

Figure S10. XPS survey spectra of **2**$(BF_4)_2$ immobilized on (111) Si (red line) and (bottom)(100) GaP (blue line). Core level photoemission associated with elemental components of the substrates (Si, Ga, P), as well as the catalyst/linker assembly (C, N, O, Ni) and counter ion (F) are observed.

References:

1) Le Goff, A.; Artero, V.; Jousselme, B.; Tran, P. D.; Guillet, N.; Metaye, R.; Fihri, A.; Palacin, S.; Fontecove, M. *Science* **2009**, 326, 1384-1387.

2) Koepp, H. M.; Wedt, H.; Strehlow, H. *Z. Elektrochem.* **1960**, 64**,** 483-491.